

LC-MS/MS-based Proteomic Analysis to Identify Protein Phosphorylation in *Emiliana huxleyi*

Van-An Duong¹, Onyou Nam^{2,3}, EonSeon Jin², Jae-Min Seo⁴, Jong-Moon Park¹, and Hookeun Lee^{1*}

¹College of Pharmacy, Gachon University, Incheon 21936, South Korea

²Department of Life Science, Research Institute for Natural Sciences, Hanyang University, Seoul 04763, South Korea

³Department of Biology, University of York, York YO10 5DD, United Kingdom

⁴Safetia Co., Ltd., Prugio-City 1st, 2 Jeongja-ro, Bundang-gu, Seongnam-si, Gyeonggi-do, South Korea

Received September 16, 2021; Revised November 04, 2021; Accepted November 04, 2021

First published on the web December 31, 2021; DOI: 10.5478/MSL.2021.12.4.163

Abstract : *Emiliana huxleyi* is a marine phytoplankton that plays a critical role in global carbon and sulfur cycling. The genome of *E. huxleyi* has been sequenced, and an in-depth proteomic profile of this organism has been reported. This study analyzed the phosphoproteome of *E. huxleyi* and identified its changes under calcium-limited conditions. A TiO₂ microcolumn was used for phosphopeptide enrichment, followed by liquid chromatography-tandem mass spectrometry analysis. Overall, we identified 7,010 phosphorylated sites on 3,355 phosphopeptides associated with 2,929 phosphoproteins in *E. huxleyi*. Quantitative analysis revealed changes in the phosphoproteome in *E. huxleyi* when ambient conditions changed to calcium-limited conditions, notably the phosphorylation of some transporters was altered. This study provides an overview of protein phosphorylation in *E. huxleyi* and paves the way for further investigations of its biological functions.

Keywords : *Emiliana huxleyi*; LC-MS/MS; proteomics; phosphorylation; calcium

Introduction

Protein phosphorylation is one of the most widespread and essential types of post-translational modifications (PTMs). It essentially influences all fundamental cellular processes, such as growth, division, differentiation, metabolism, organelle trafficking, motility, muscle contraction, membrane transport, immunity, learning, and memory.^{1,2} The phosphorylation of proteins is the transfer of a phosphate group from adenosine triphosphate (ATP) to specific amino acids in proteins mediated by protein kinases.³ In eukaryotes, protein phosphorylation usually occurs in Ser, Thr, and Tyr residues. After the addition of phosphate groups, proteins change from a hydrophobic apolar to hydrophilic polar form, allowing them to interact more

easily with other molecules.⁴ Mass spectroscopy-based proteomics is an indispensable technique to study biology.⁵⁻⁷ It is powerful to profile a large number of proteins in a sample.⁸ Proteomics is also used to investigate protein PTMs, including phosphorylation.⁹ A typical workflow for a bottom-up phosphoproteomic study includes protein digestion, phosphopeptide enrichment, and liquid chromatography-tandem mass spectrometry (LC-MS/MS) analysis. Since phosphopeptides are less abundant than other peptides in the initial proteins, phosphopeptide enrichment is critical before sample analysis.

Emiliana huxleyi is a unicellular marine phytoplankton distributed throughout the ocean. It belongs to the coccolithophores group and has a unique morphology.¹⁰ *E. huxleyi* has been studied for application in various fields, such as biogeography, geology, material science, medicine, ecophysiology, and paleoclimatology.¹¹ As a coccolithophore, *E. huxleyi* can fix inorganic carbon into biomineralized and photosynthetic products via photosynthesis and calcification.¹² Consequently, it produces calcium carbonate mineral plates on exoskeletons called coccoliths¹³, forming chalk and limestone sediments.¹⁴ Therefore, *E. huxleyi* plays a crucial role in global carbon and sulfur cycling.¹⁵ Furthermore, it contributes to marine cloud formation and climate regulation.^{14,16} The blooms formed by *E. huxleyi* can cover areas up to 250,000 km² on the ocean surface.

In 2013, Read et al. reported the genome sequence database of *E. huxleyi* CCMP 1516 with 30,569 protein-

Open Access

*Reprint requests to Hookeun Lee

<https://orcid.org/0000-0002-0696-8421>

E-mail: hklee@gachon.ac.kr

All the content in Mass Spectrometry Letters (MSL) is Open Access, meaning it is accessible online to everyone, without fee and authors' permission. All MSL content is published and distributed under the terms of the Creative Commons Attribution License (<http://creativecommons.org/licenses/by/3.0/>). Under this license, authors reserve the copyright for their content; however, they permit anyone to unrestrictedly use, distribute, and reproduce the content in any medium as far as the original authors and source are cited. For any reuse, redistribution, or reproduction of a work, users must clarify the license terms under which the work was produced.

coding genes.¹⁷ Several researchers performed proteomic studies of this species with a limited number of identified proteins. Jones et al. studied *E. huxleyi* NZEH using one-dimensional sodium dodecyl sulfate-polyacrylamide gel electrophoresis (SDS-PAGE) and LC-MS/MS and identified 99 proteins.¹⁸ Later, the same group used two-dimensional LC and identified 115 homologous protein groups.¹⁹ Approximately 500 proteins were found in other LC-MS/MS-based proteomic studies.^{20,21} Recently, we developed a three-dimensional platform consisting of strong cation exchange fractionation, high pH reversed-phase LC fractionation, and low pH reversed-phase LC-MS/MS analysis for the in-depth proteomic profiling of *E. huxleyi* CCMP371.²² We identified more than 15,000 protein groups (including single hits) in 70 fractions. The dataset obtained has been used for the global discovery of PTMs.²³ A total of 13,483 PTMs belonging to 25 different PTM types were identified in 7,421 proteins, which increased the protein identification to 18,780. In another study, we investigated the *de novo* transcriptome profile of *E. huxleyi* CCMP371 at different calcium concentrations and observed calcium-associated regulation at the molecular level.²⁴

This study aimed to identify protein phosphorylation in *E. huxleyi* CCMP371 and evaluate the effects of calcium-limited conditions on the phosphoproteome of this species. We used a typical bottom-up proteomics workflow consisting of protein digestion, phosphopeptide enrichment with a TiO₂ microcolumn, and LC-MS/MS analysis. This is the first study on the phosphoproteome of *E. huxleyi* CCMP371, which is useful for future studies on this species.

Experimental

Materials

Ammonium bicarbonate, formic acid (FA), and iodoacetamide (IAA) were purchased from Sigma-Aldrich (St. Louis, MO, USA). Sequencing-grade modified trypsin was purchased from Promega (Madison, WI, USA). Tris (2-carboxyethyl) phosphine (TCEP) was obtained from Thermo Fisher Scientific (Rockford, IL, USA). HPLC-grade water and acetonitrile (ACN) were obtained from J.T. Baker (Phillipsburg, NJ, USA). All chemicals were of analytical grade and were used as received without further purification.

Cell culture

E. huxleyi CCMP371 was purchased from the Provasoli-Guillard National Center for Marine Algae and Microbiota (NCMA, East Boothbay, ME, USA). Cells were cultured in sterile artificial seawater at 20 ± 1°C under a 12:12 h light:dark cycle with an irradiance of 50 μmol m⁻²s⁻¹. The artificial seawater was enriched with phosphates, nitrates, trace metals, vitamins at f/2 concentration, and selenium.^{25,26} The ambient calcium concentration (Ca²⁺) was 10 mM. To induce calcium-limited conditions, cells

cultured at an ambient calcium concentration were collected and centrifuged to remove the remaining medium. Subsequently, the cells were inoculated in a fresh medium with a calcium concentration of 0.1 mM. Cells acclimated under these conditions were sub-cultured in fresh medium with 0.1 mM Ca²⁺ for more than 20 generations.²⁴ Cell pellets from two conditions (10 mM Ca²⁺ and 0.1 mM Ca²⁺) were collected for proteomic analysis (*n* = 3).

Proteomic analysis

Protein extraction and digestion

Protein extraction from cell pellets was performed as described in a previous report.²⁷ Briefly, the cell pellets were placed in Maintainer[®] Tissue cards for heat stabilization at 95°C in Stabilizer[™] T1 (Denator AB, Gothenburg, Sweden) to stop degradation. Subsequently, the samples were loaded into pre-chilled TT1 tissue TUBE[™] (Covaris, Woburn, MA, USA) and frozen in liquid nitrogen before pulverization using CryoPrep[®] (Covaris). Lysis buffer (8 M urea and 0.1 M Tris-HCl, pH 8.5) was added to the sample, followed by sonication for 12 min at 18°C (Covaris). Proteins were extracted using the acetone precipitation method. Briefly, the samples were mixed with four volumes of acetone (pre-chilled at -20°C), incubated at -20°C for 18 h, and centrifuged at 4,000 rpm for 10 min at 4°C (Centrifuge 5810 R; Eppendorf, Hamburg, Germany). After discarding the supernatant, the protein pellets were collected, washed with acetone, and subsequently dried in a ScanSpeed 40 centrifugal evaporator at 1,800 rpm for 3 h (Labogene, Lillerød, Denmark). The proteins were resuspended in lysis buffer, and the protein amount was quantified using the Pierce BCA Protein Assay kit (Thermo Fisher Scientific).

Protein digestion was carried out using filter-aided sample preparation (FASP) with Ultracel[®] YM-30 centrifugal filters (Merck Millipore, Darmstadt, Germany).^{28,29} Proteins (100 μg/100 μL) were reduced with 1 μL of 500 mM TCEP at 37°C for 30 min. Subsequently, the samples were alkylated with 10 μL of 500 mM IAA at 25°C for 30 min in the dark and digested with trypsin at 37°C for 18 h at an enzyme to protein ratio of 1:50. After digestion, the peptide mixtures were collected. Thereafter, FA was added to inactivate the trypsin, after which C₁₈ microspin columns (Harvard Apparatus, MA, USA) were used for sample desalting. The samples were then concentrated by vacuum drying at 1,800 rpm for 3 h (ScanSpeed 40 centrifugal evaporator).

Phosphopeptide enrichment

After desalting, the peptides were reconstituted in 0.1% FA/water (solvent A). A TiO₂ microcolumn (TitanspherePhos-TiO kit; GL Sciences, Tokyo, Japan) was used for phosphopeptide enrichment. The column was conditioned in solvent B (2% trifluoroacetic acid solution: ACN [20:80, v/v]) and equilibrated in solvent C (lactic acid: solvent B [25:75, v/v]). Samples

were loaded into the microcolumn, and 100 μL of solvent C was added, followed by slow pipetting for mixing. Non-phosphopeptides were removed by centrifugation at 3,000 rpm for 10 min. Next, solvents C and B were added for rinsing. Phosphopeptides were then eluted with 50 μL of 5% ammonium hydroxide, followed by 50 μL of 5% pyrrolidine (1,000 rpm, 5 min). After drying, the enriched phosphopeptides were reconstituted in 50 μL of solvent A (0.1% FA/water) and injected (1 μg) to an LC-MS/MS system for analysis.

LC-MS/MS analysis

LC-MS/MS analysis of the samples was similar to that conducted in a previous study.²⁹ The LC-MS/MS system consisted of a Dionex Ultimate 3000 HPLC coupled with a Q Exactive™ Hybrid Quadrupole-Orbitrap mass spectrometer (Thermo Fisher Scientific). The samples were loaded onto an Acclaim™ PepMap™ 100 C18 nano-trap column (75 $\mu\text{m} \times 2 \text{ cm}$, 3 μm particles, 100-Å pores; Thermo Fisher Scientific) using solvent A at a flow rate of 2.5 $\mu\text{L}/\text{min}$ for 5 min. Peptide separation was conducted using an Acclaim™ PepMap™ C18 100A RSLC nano-column (75 $\mu\text{m} \times 50 \text{ cm}$, 2 μm particles, 100-Å pores; Thermo Fisher Scientific). The mobile phase solvent consisted of solvents A and B (0.1% FA in ACN: water [80:20, v/v]), and the flow rate was fixed at 300 nL/min. The gradient was set up as follows: solvent B, equilibration at 4% for 14 min, 4–20% for 61 min, 20–50% for 81 min, 50–96% for 1 min, holding at 96% for 10 min, 96–4% for 1 min, and holding at 4% for 17 min for column re-equilibration. The operation parameters were as follows: spray voltage, 2.2 kV; capillary temperature, 320°C; isolation width, $\pm 2 m/z$; scan range, 400–2,000 m/z ; resolution of full-MS scans, 70,000; and resolution of MS/MS scans at 200 m/z , 17,500. A data-dependent acquisition method was used, wherein the top ten precursor ions with the highest intensity were isolated in the quadrupole and fragmented by the higher-energy collisional dissociation with 27% normalized collisional energy. Dynamic exclusion was set at 20 s to minimize repeated analyses of the same abundant precursor ions.

Data analysis

For phosphopeptide identification, raw MS/MS data files were converted to mzXML format using MSConvert. Comet (version 2017.01 rev.0) was used to search MS/MS spectra against the Uniprot database of *E. huxleyi* (CCMP371). The following parameters were set for the search: maximum of two missed cleavages with trypsin; semitryptic cleavage, 10 ppm and 0.02 Da tolerances for precursor ion masses and fragment ion masses, respectively; static carbamidomethylation of cysteine; and variable modifications including oxidation (methionine, +15.995 Da), carbamylation (protein N-term, +43.0006 Da), and phosphorylation (serine, threonine, and tyrosine, +79.9663

Da). The search result files in pepXML format were transferred to Trans-Proteomic Pipeline (TPP) version 5.1.0,³⁰ and PeptideProphet³¹ was run. The peptides were filtered at a false discovery rate (FDR) of ≤ 0.01 .

Phosphopeptide quantification was carried out using MaxQuant version 1.5.8.3 (www.coxdocs.org) with the Andromeda search engine.³² The parameters were set as follows: maximum of two missed cleavages with trypsin, 20 ppm for first search peptide tolerance, 4.5 ppm for main search peptide tolerance, and an FDR cutoff of 1%. Fixed and variable modifications were the same as those in the Comet search. The data were analyzed and visualized using Mass Profiler Professional version 12.6.1 (Agilent Technologies, Santa Clara, CA, USA). A Student's *t*-test with a Benjamini–Hochberg correction was used for statistical analysis. Missing values were kept and a quantile normalization was performed. Differentially expressed

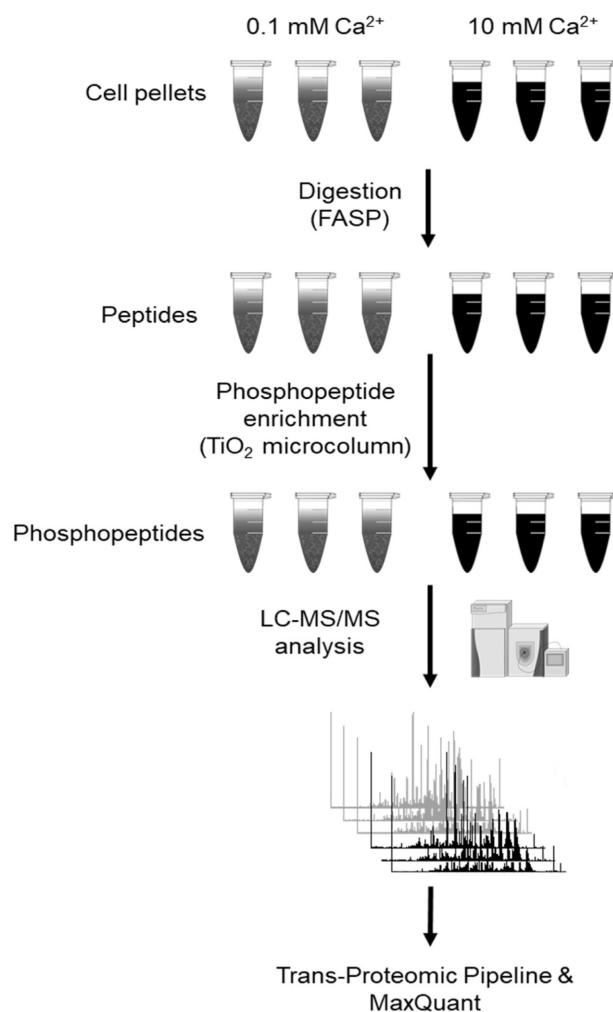


Figure 1. Workflow of phosphoproteomic analysis of *E. huxleyi* CCMP371 using FASP digestion, phosphopeptide enrichment, and LC-MS/MS analysis.

phosphopeptides were identified with a corrected p -value ≤ 0.05 and a fold-change ≥ 2 . Gene Ontology (GO)³³ and Kyoto Encyclopedia of Gene and Genomes (KEGG) pathway³⁴ were categorized using Cytoscape version 3.7.2 (National Institute of General Medical Sciences, Bethesda, MD, USA) via ClueGO version 2.5.6 (Cordeliers Research Center, Paris, France).³⁵ The GO terms and KEGG pathways were filtered at a p -value ≤ 0.05 .

Results and Discussion

In a previous study, we used a three-dimensional LC combined with MS/MS analysis for the in-depth proteomic profiling of *E. huxleyi*, which allowed the discovery of the phosphoproteome in this species without an enrichment method.²³ We previously identified 1,120 phosphorylated sites on 789 proteins, which was relatively low compared with those in recent phosphoproteomic studies.³⁶ Therefore, in the present study, we performed a typical bottom-up proteomics workflow to profile the phosphoproteome of *E. huxleyi* CCMP371. As shown in Figure 1, after digestion using FASP, phosphopeptides were enriched with a TiO₂ microcolumn before LC-MS/MS analysis. TPP with Comet search was used for phosphopeptide identification, and MaxQuant was employed for comparative analysis between phosphoproteomes under ambient and calcium-limited conditions.

Identification of protein phosphorylation in *E. huxleyi* CCMP371

Using TPP with a Comet search, we identified 4,200 peptides from all samples. Among them, there were 3,355 phosphopeptides (Table S1) associated with 2,929 proteins and protein groups (hereafter, for simplification, “protein” is used to denote both proteins and protein groups). The enrichment efficacy was approximately 80%. From these phosphopeptides, 7,158 phosphorylated sites were identified. However, some phosphorylated sites that overlapped were manually removed, finally resulting in 7,010 phosphorylated sites. The numbers of phosphorylated sites and phosphoproteins were 6.3- and 3.7-fold higher, respectively, than those obtained in a previous study.²³ However, the numbers of identified phosphorylated sites and phosphoproteins were relatively lower than those in other species, such as *Saccharomyces cerevisiae* (40,000 phosphorylated sites in 3,000 phosphoproteins), *Mus musculus* (156,000 phosphorylated sites in 11,000 phosphoproteins), and *Homo sapiens* (230,000 phosphorylated sites in 13,000 phosphoproteins).³⁷

Figure 2 summarizes the results of the phospho-proteomic profiling of *E. huxleyi* in the present study. The number of phosphopeptides per protein varied from 1 to 13 (Figure 2a), with the majority (~89%) of phosphoproteins having one phosphopeptide. The number of phosphorylated sites per protein ranged from 1 to 26. Approximately 93% of the

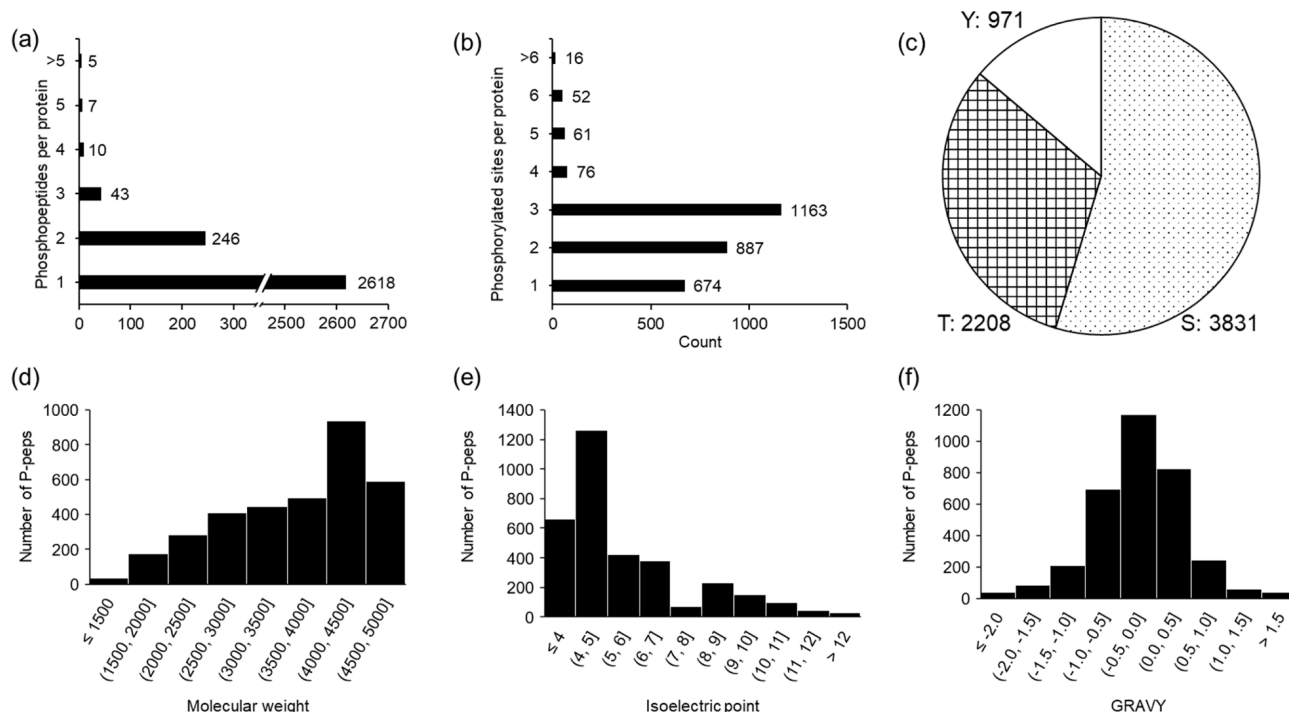


Figure 2. Identification of phosphopeptides using the Trans-Proteomic Pipeline with Comet search. (a) Number of phosphopeptides identified per protein. (b) Number of phosphorylated sites identified per protein. (c) Number of phosphorylated Ser (S), Thr (T), and Tyr (Y) identification. (d, e, f) Distribution of molecular weight, isoelectric point (pI), and grand average of hydropathy (GRAVY) values of identified phosphopeptides. P-peps: phosphopeptides.

phosphoproteins contained 1–3 phosphorylated sites (Figure 2b). Notably, in protein R1D509 (polyketide synthase), we identified 13 phosphopeptides and 26 phosphorylated sites. Among the 7,010 phosphorylated sites, serine accounted for more than 54%, while threonine accounted for approximately 31.5% (Figure 2c). We found a ratio of 55:31:14 for Ser/Thr/Tyr in *E. huxleyi*, which was close to the ratio of 70:20:10 in *Bacillus subtilis* and relatively different from the ratio of 86:12:2 in humans.³⁸

The physicochemical properties of the identified phosphopeptides were also assessed. The molecular weight (MW) and isoelectric point (pI) of the phosphopeptides were obtained from TPP. The pI value of a peptide is the pH at which it carries no net charge. The grand average of hydropathy (GRAVY) values of peptides were calculated using the GRAVY calculator to signify the hydrophilicity (GRAVY<0) or hydrophobicity (GRAVY>0).³⁹ As shown in Figure 2d, the majority of the identified phosphopeptides had MW >3,000 Da (73%), pI <7 (81%), and GRAVY between -1 and 0.5 (80%).

Next, we used Cytoscape via ClueGO to categorize 2,929 phosphoproteins based on the GO database of *E. huxleyi* (updated on October 31, 2019). We identified 93 biological processes, 8 cellular components, and 73 molecular functions with a *p*-value ≤0.05, and the number of genes was found to be ≥3 (Table S2). As shown in Figure 3, most of the identified GO terms had less than 40% associated genes. The top five GO terms with the lowest *p*-values are listed in Table 1. Typical biological processes associated with phosphopeptides were transmembrane transport and metabolic

and biosynthetic processes. These phosphopeptides are components of non-membrane-bound organelles and plasma membrane protein complexes. In addition, they are involved in binding functions and passive transmembrane transporter activity (Table S2).

Effects of calcium concentration on phosphoproteome of *E. huxleyi* CCMP371

We also evaluated the effects of calcium concentration

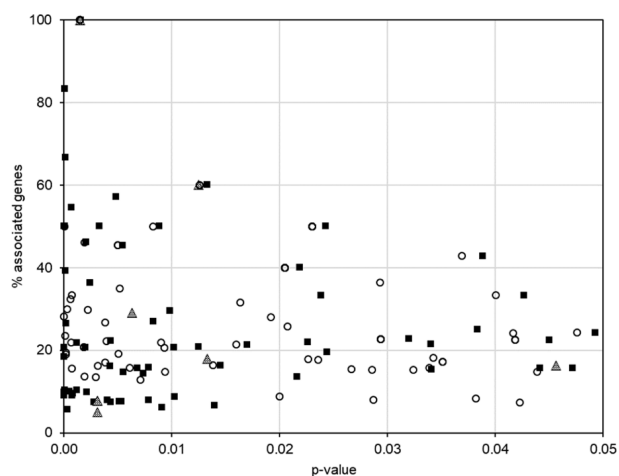


Figure 3. Gene ontology terms associated with phosphoproteins of *Emiliana huxleyi*. The data were obtained using Cytoscape via ClueGO. ■: biological processes; ▲: cellular components; ○: molecular functions.

Table 1. Top 5 GO terms with lowest *p*-value.

GO ID	GO term	<i>p</i> -value	Number of gene found
Biological processes			
GO:0044267	Cellular protein metabolic process	1.5×10^{-6}	229
GO:0005975	Carbohydrate metabolic process	8.3×10^{-6}	92
GO:0007165	Signal transduction	2.2×10^{-5}	54
GO:0005976	Polysaccharide metabolic process	2.8×10^{-5}	10
GO:0043412	Macromolecule modification	3.0×10^{-5}	204
Cellular components			
GO:0000148	1,3-beta-D-glucan synthase complex	1.5×10^{-3}	3.00
GO:0005739	Mitochondrion	3.1×10^{-3}	9.00
GO:0043228	Non-membrane-bounded organelle	3.1×10^{-3}	46.00
GO:0098797	Plasma membrane protein complex	3.1×10^{-3}	9.00
GO:0008278	Cohesin complex	6.3×10^{-3}	3.00
Molecular functions			
GO:0071949	FAD binding	1.9×10^{-5}	24.00
GO:0002161	Aminoacyl-tRNA editing activity	6.2×10^{-5}	9.00
GO:0016810	Hydrolase activity, acting on carbon-nitrogen (but not peptide) bonds	1.2×10^{-4}	30.00
GO:0004553	Hydrolase activity, hydrolyzing O-glycosyl compounds	1.5×10^{-4}	50.00
GO:0016798	Hydrolase activity, acting on glycosyl bonds	1.8×10^{-4}	53.00

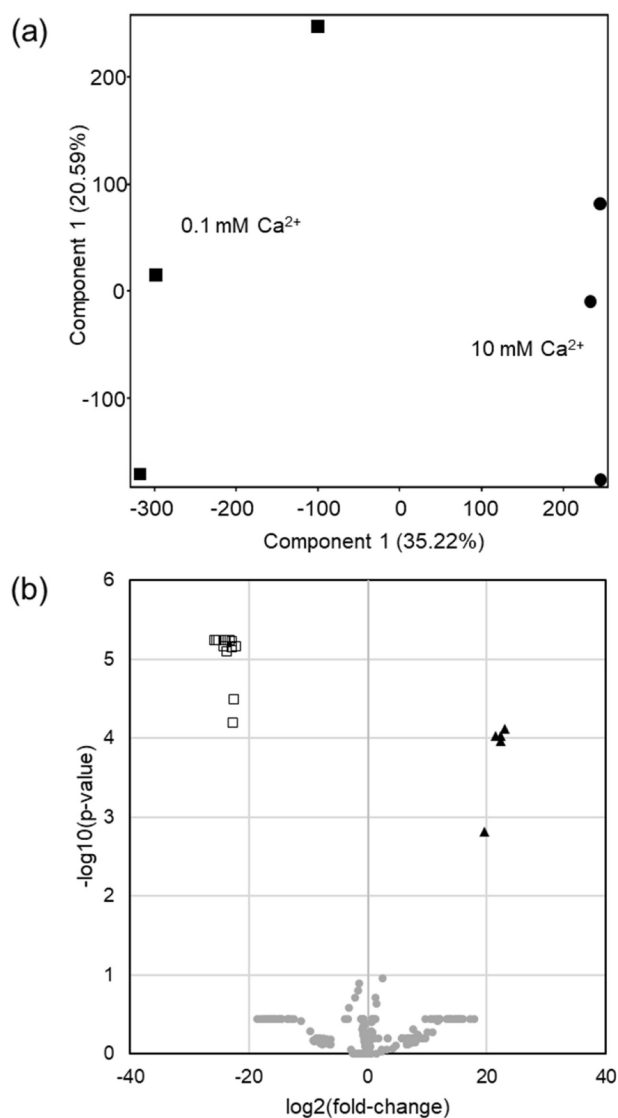


Figure 4. Comparative analysis of phosphoproteome between calcium-limited and ambient conditions. (a) Principal component analysis. ■: calcium-limited condition (0.1 mM Ca²⁺); ●: ambient condition (10 mM Ca²⁺). (b) Volcano plot (calcium-limited condition *versus* ambient condition) of 291 phosphopeptides. ▲: up-regulated phosphopeptides; □: down-regulated phosphopeptides; ●: un-regulated phosphopeptides.

on the phosphoproteome of *E. huxleyi* by culturing the cells in ambient (10 mM Ca²⁺) and calcium-limited (0.1 mM Ca²⁺) conditions for phosphoproteome profiling ($n=3$). Using MaxQuant, we quantified 400 phosphopeptides (Table S3). Next, we selected 291 phosphopeptides found in at least 2 of the 6 samples and used Mass Profiler Professional to analyze them statistically. Principal component analysis (Figure 4a) revealed separation between the two groups. Components 1, 2, 3, and 4 contributed 35.22%, 20.59%, 17.03%, and 14.16% of the total variance, respectively. A

volcano plot of 291 phosphopeptides (calcium-limited *versus* ambient conditions) is shown in Figure 4b. As a result, 5 phosphopeptides associated with 4 phosphoproteins were upregulated, and 13 phosphopeptides associated with 11 phosphoproteins were downregulated under calcium-limited conditions (Table 2). In addition, we identified 105 phosphopeptides associated with 88 proteins that were only quantified under calcium-limited conditions (up-phosphorylation group) and 72 phosphopeptides associated with 55 proteins that were only quantified under ambient conditions (down-phosphorylation group) (Table S4). The differentially expressed phosphopeptides are listed in Table 2. After removing the six proteins that appeared in both groups, we used these proteins to investigate the effects of calcium-limited conditions on the phosphoproteome of *E. huxleyi*.

We used Cytoscape via ClueGo to categorize phosphoproteins based on the GO database of *E. huxleyi* and identified terms with a p -value ≤ 0.05 and the number of genes found ≥ 1 . The phosphoproteins were those associated with differentially expressed phosphopeptides (Table 2) and exclusively quantified phosphopeptides in each group (Table S4). A total of 66 biological processes, 7 cellular components, and 32 molecular functions were found in the up-phosphorylation group, whereas 60 biological processes, 8 cellular components, and 30 molecular functions were found in the down-phosphorylation group (Table S5). Under calcium-limited conditions, there was an increase in the phosphorylation of some proteins associated with transmembrane transporter activity (six proteins), regulation of macromolecule metabolic processes (five proteins), nucleobase-containing compound transport (three proteins), other transporter activities (anion and carbohydrate derivatives), and RNA splicing. In contrast, there were decreases in the phosphorylation of proteins associated with hydrolase activity (eight proteins), pyrophosphatase activity (eight proteins), nucleoside-triphosphatase activity (seven proteins), transmembrane transport (five proteins), non-membrane-bounded organelle (four proteins), and other transporter and binding activities were observed. Notably, the phosphorylation levels of the Na⁺/Ca²⁺-K⁺ exchanger (RIDUD8) and ammonium transporter (RIDMV7) decreased.

Protein phosphorylation is crucial for eukaryotic cells because it regulates cellular metabolism, enzymatic reactions, protein–protein interactions, protein degradation, and more importantly, photosynthetic acclimation to the environment.^{3,40} In *E. huxleyi*, we previously reported a low number of phosphorylated sites (1,120) and phosphoproteins (789). The enrichment with the TiO₂ microcolumn remarkably increased the number of phosphorylated sites and phosphoproteins. However, these were still relatively low compared with those in yeast, mice, and humans.

Under calcium-limited conditions, coccolith formation was inhibited; however, *E. huxleyi* grew undisturbed.²⁴ It has been previously found that under calcium-limited

Table 2. Differentially expressed phosphopeptides in calcium-limited condition.

Peptide sequence	Protein	Corrected <i>p</i> -value	Fold-change
Up-regulation			
LEEPEVVTRRKTLAASPSAGSIDGRYTEKAP	R1FET8	9.3×10 ⁻⁵	5.5×10 ⁶
GFSLFQCGDASARSASPPDSPRRNARSIQR	R1FQN2	9.3×10 ⁻⁵	2.9×10 ⁶
ACASYLREKLLPGSATNLARAAATSN	R1B792	1.5×10 ⁻³	7.8×10 ⁵
SLHKRPTSFFLSRANTFLSFKPKQRDAVAVA	R1FFI3	7.6×10 ⁻⁵	9.1×10 ⁶
GGQPGGSSASLHKRPTSFFLSRANTFLSFKP	R1FFI3	1.1×10 ⁻⁴	5.7×10 ⁶
Down-regulation			
IQEEAETADAESIRRSVAEEEEATQRAIEEE	R1BSA7	5.9×10 ⁻⁶	7.3×10 ⁶
MSGDTLTSYQDAEEAL	R1BY48	6.6×10 ⁻⁵	6.3×10 ⁶
MSGEEPTLPPGEEAAEDH	R1CP36	5.9×10 ⁻⁶	4.2×10 ⁷
DRRTWRPATGRAATASEAEGEASAAARKTPK	R1FIJ5	5.9×10 ⁻⁶	3.4×10 ⁷
ATGRAATASEAEGEASAAARKTPKKGKEPKI	R1FIJ5	5.9×10 ⁻⁶	5.2×10 ⁷
GGSENFRRGSAVARDPSVSSEAPKKKKAKPPP	R1F5Y2	7.1×10 ⁻⁶	7.2×10 ⁶
TPSTDVEIGGIRTRGSFQAGQSETRYSVRTK	R1E1S3	5.9×10 ⁻⁶	9.7×10 ⁶
MSQADWLEQNVERISKD	R1EGY0	6.9×10 ⁻⁶	2.0×10 ⁷
KPPTSAGKSRSLRELSGEAKAKAAAAASTAQE	R1EWW1	8.1×10 ⁻⁶	1.4×10 ⁷
FKPLDAATKANLPHKSFRRSYAYAVMDETKS	R1FFT9	6.9×10 ⁻⁶	4.7×10 ⁶
DAATKANLPHKSFRRSYAYAVMDETKSSTSY	R1FFT9	5.9×10 ⁻⁶	1.5×10 ⁷
AAGRGLKKSRSKRSATSLQSGSGLLRSSQR	R1EBL1	3.2×10 ⁻⁵	5.6×10 ⁶
VELMGEPVKLTVGEYTNLKLTPEDMIAET	R1ETX0	5.9×10 ⁻⁶	1.6×10 ⁷

conditions, *E. huxleyi* exhibits some changes in the expression of calcium transporters, inorganic transporters, and ATP-binding cassette family transporters.²⁴ In the present study, we found a reduction in the phosphorylation of the Na⁺/Ca²⁺-K⁺ exchanger and ammonium transporter as well as alterations in phosphorylation of other transporter and binding proteins. However, since many proteins in *E. huxleyi* have not been characterized, the interpretation of the resulting dataset is currently insufficient. It is expected that when the proteome of this species is extensively studied, a re-analysis of this dataset will reveal more information on its acclimation to the environment by altering the phosphoproteome.

Conclusions

Here, we identified the phosphoproteomic profile of *E. huxleyi* with 7,010 phosphorylated sites on 2,929 proteins. Enriched GO terms from the phosphoproteins included transmembrane transport, metabolic and biosynthetic processes, plasma membrane protein complex, some binding functions, and passive transmembrane transporter activity. In addition, we revealed changes in the phosphoproteome of *E. huxleyi* under calcium-limited conditions. Notably, there were alterations in the phosphorylation of the Na⁺/Ca²⁺-K⁺ exchanger, ammonium transporter, other transporters, and binding proteins.

Supplementary Information

Supplementary Information is available at <https://drive.google.com/file/d/10AVP1nACa7EryTC2YVOAsL0ydBBDSSRg/view?usp=sharing>.

Acknowledgments

This research was supported by the National Research Foundation of Korea (NRF) grant, funded by the Korean government (MSIT) (No. NRF-2017M3D9A1073784, NRF- 2020R1I1A1A01074257).

References

- Manning, G.; Whyte, D. B.; Martinez, R.; Hunter, T.; Sudarsanam, S. *Science* **2002**, 298, 1912, DOI: 10.1126/science.1075762.
- Manning, G.; Plowman, G. D.; Hunter, T.; Sudarsanam, S. *Trends Biochem. Sci.* **2002**, 27, 514, DOI: 10.1016/s0968-0004(02)02179-5.
- Ubersax, J. A.; Ferrell Jr, J. E. *Nat. Rev. Mol. Cell Biol.* **2007**, 8, 530, DOI: 10.1038/nrm2203.
- Ardito, F.; Giuliani, M.; Perrone, D.; Troiano, G.; Lo Muzio, L. *Int. J. Mol. Med.* **2017**, 40, 271, 10.3892/ijmm.2017.3036.
- Aebersold, R.; Mann, M. *Nature* **2003**, 422, 198, DOI: 10.1038/nature01511.

6. Tyers, M.; Mann, M. *Nature* **2003**, 422, 193, DOI: 10.1038/nature01510.
7. Duong, V.-A.; Park, J.-M.; Lim, H.-J.; Lee, H. *Appl. Sci.* **2021**, 11, 3393, DOI: 10.3390/app11083393.
8. Duong, V.-A.; Park, J.-M.; Lee, H. *Int. J. Mol. Sci.* **2020**, 21, 1524, DOI: 10.3390/ijms21041524.
9. Zhang, P.; He, W.; Huang, Y.; Xiao, K.; Tang, Y.; Huang, L.; Huang, X.; Zhang, J.; Yang, W.; Liu, R.; Fu, Q.; Lu, Y.; Zhang, M. *Theriogenology* **2021**, 170, 1, DOI: 10.1016/j.theriogenology.2021.04.013.
10. Cubillos, J.; Wright, S.; Nash, G.; De Salas, M.; Griffiths, B.; Tilbrook, B.; Poisson, A.; Hallegraeff, G. *Mar. Ecol. Prog. Ser.* **2007**, 348, 47, DOI: 10.3354/meps07058.
11. Totti, C.; Romagnoli, T.; Accoroni, S.; Coluccelli, A.; Pellegrini, M.; Campanelli, A.; Grilli, F.; Marini, M. *J. Mar. Syst.* **2019**, 193, 137, DOI: 10.1016/j.jmarsys.2019.01.007.
12. Iglesias-Rodríguez, M. D.; Brown, C. W.; Doney, S. C.; Kleypas, J.; Kolber, D.; Kolber, Z.; Hayes, P. K.; Falkowski, P. G. *Global Biogeochem. Cycles* **2002**, 16, 47, DOI: 10.1029/2001GB001454.
13. Obata, T.; Shiraiwa, Y. *J. Biol. Chem.* **2005**, 280, 18462, DOI: 10.1074/jbc.M501517200.
14. Paasche, E. *Phycologia* **2001**, 40, 503, DOI: 10.2216/i0031-8884-40-6-503.1.
15. Hallegraeff, G. M. *J. Phycol.* **2010**, 46, 220, DOI: 10.1111/j.1529-8817.2010.00815.x.
16. Rost, B.; Riebesell, U.; Burkhardt, S.; Sültemeyer, D. *Limnol. Oceanogr.* **2003**, 48, 55, DOI: 10.4319/lo.2003.48.1.0055.
17. Read, B. A.; Kegel, J.; Klute, M. J.; Kuo, A.; Lefebvre, S. C.; Maumus, F.; Mayer, C.; Miller, J.; Monier, A.; Salamov, A.; Young, J.; Aguilar, M.; Claverie, J.-M.; Frickenhaus, S.; Gonzalez, K.; Herman, E. K.; Lin, Y.-C.; Napier, J.; Ogata, H.; Sarno, A. F.; Shmutz, J.; Schroeder, D.; de Vargas, C.; Verret, F.; von Dassow, P.; Valentin, K.; Van de Peer, Y.; Wheeler, G.; *Emiliania huxleyi* Annotation, C.; Allen, A. E.; Bidle, K.; Borodovsky, M.; Bowler, C.; Brownlee, C.; Mark Cock, J.; Elias, M.; Gladyshev, V. N.; Groth, M.; Guda, C.; Hadaegh, A.; Debora Iglesias-Rodríguez, M.; Jenkins, J.; Jones, B. M.; Lawson, T.; Leese, F.; Lindquist, E.; Lobanov, A.; Lomsadze, A.; Malik, S.-B.; Marsh, M. E.; Mackinder, L.; Mock, T.; Mueller-Roeber, B.; Pagarete, A.; Parker, M.; Probert, I.; Quesneville, H.; Raines, C.; Rensing, S. A.; Riaño-Pachón, D. M.; Richier, S.; Rokitta, S.; Shiraiwa, Y.; Soanes, D. M.; van der Giezen, M.; Wahlund, T. M.; Williams, B.; Wilson, W.; Wolfe, G.; Wurch, L. L.; Dacks, J. B.; Delwiche, C. F.; Dyhrman, S. T.; Glöckner, G.; John, U.; Richards, T.; Worden, A. Z.; Zhang, X.; Grigoriev, I. V. *Nature* **2013**, 499, 209, DOI: 10.1038/nature12221.
18. Jones, B. M.; Edwards, R. J.; Skipp, P. J.; O'Connor, C. D.; Iglesias-Rodríguez, M. D. *Mar. Biotechnol.* **2011**, 13, 496, DOI: 10.1007/s10126-010-9320-0.
19. Jones, B. M.; Iglesias-Rodríguez, M. D.; Skipp, P. J.; Edwards, R. J.; Greaves, M. J.; Young, J. R.; Elderfield, H.; O'Connor, C. D. *PLoS One* **2013**, 8, e61868, DOI: 10.1371/journal.pone.0061868.
20. McKew, B. A.; Lefebvre, S. C.; Achterberg, E. P.; Metodieva, G.; Raines, C. A.; Metodiev, M. V.; Geider, R. J. *New Phytol.* **2013**, 200, 61, DOI: 10.1111/nph.12352.
21. McKew, B. A.; Metodieva, G.; Raines, C. A.; Metodiev, M. V.; Geider, R. J. *Environ. microbiol.* **2015**, 17, 4050, DOI: 10.1111/1462-2920.12957.
22. Yun, G.; Park, J.-M.; Duong, V.-A.; Mok, J.-H.; Jeon, J.; Nam, O.; Lee, J.; Jin, E.; Lee, H. *Molecules* **2020**, 25, 3028, DOI: 10.3390/molecules25133028.
23. Duong, V.-A.; Nam, O.; Jin, E.; Park, J.-M.; Lee, H. *Molecules* **2021**, 26, 2027, DOI: 10.3390/molecules26072027.
24. Nam, O.; Park, J.-M.; Lee, H.; Jin, E. *PLoS One* **2019**, 14, e0221938, DOI: 10.1371/journal.pone.0221938.
25. Guillard, R. R. L. 1975. Culture of Phytoplankton for Feeding Marine Invertebrates. In *Culture of Marine Invertebrate Animals: Proceedings — 1st Conference on Culture of Marine Invertebrate Animals Greenport*. W.L. Smith, and M.H. Chanley, editors. Boston, MA: Springer US. 29.
26. Araie, H.; Sakamoto, K.; Suzuki, I.; Shiraiwa, Y. *Plant Cell Physiol.* **2011**, 52, 1204, DOI: 10.1093/pcp/pcr070.
27. Kwon, D.; Park, J.-M.; Duong, V.-A.; Hong, S.-J.; Cho, B.-K.; Lee, C.-G.; Choi, H.-K.; Kim, D.-M.; Lee, H. *J. Mar. Sci. Eng.* **2020**, 8, 790, DOI: 10.3390/jmse8100790.
28. Wisniewski, J. R.; Zougman, A.; Nagaraj, N.; Mann, M. *Nat. Methods* **2009**, 6, 359, DOI: 10.1038/nmeth.1322.
29. Koh, K.; Park, M.; Bae, E. S.; Duong, V.-A.; Park, J.-M.; Lee, H.; Lew, H. *Stem Cell Res. Ther.* **2020**, 11, 428, DOI: 10.1186/s13287-020-01943-w.
30. Deutsch, E. W.; Mendoza, L.; Shteynberg, D.; Slagel, J.; Sun, Z.; Moritz, R. L. *Proteomics Clin. Appl.* **2015**, 9, 745, doi.org/10.1002/prca.201400164.
31. Keller, A.; Nesvizhskii, A. I.; Kolker, E.; Aebersold, R. *Anal. Chem.* **2002**, 74, 5383, DOI: 10.1021/ac025747h.
32. Cox, J.; Mann, M. *Nat. Biotechnol.* **2008**, 26, 1367, DOI: 10.1038/nbt.1511.
33. Ashburner, M.; Ball, C. A.; Blake, J. A.; Botstein, D.; Butler, H.; Cherry, J. M.; Davis, A. P.; Dolinski, K.; Dwight, S. S.; Eppig, J. T.; Harris, M. A.; Hill, D. P.; Issel-Tarver, L.; Kasarskis, A.; Lewis, S.; Matese, J. C.; Richardson, J. E.; Ringwald, M.; Rubin, G. M.; Sherlock, G. *Nat. Genet.* **2000**, 25, 25, DOI: 10.1038/75556.
34. Kanehisa, M.; Goto, S.; Kawashima, S.; Nakaya, A. *Nucleic Acids Res.* **2002**, 30, 42, DOI: 10.1093/nar/30.1.42.
35. Bindea, G.; Mlecnik, B.; Hackl, H.; Charoentong, P.; Tosolini, M.; Kirilovsky, A.; Fridman, W.-H.; Pagès, F.; Trajanoski, Z.; Galon, J. *Bioinformatics* **2009**, 25, 1091, DOI: 10.1093/bioinformatics/btp101.
36. Li, J.; Paulo, J. A.; Nusinow, D. P.; Huttlin, E. L.; Gygi, S. P. *Cell Rep.* **2019**, 29, 2092, DOI: 10.1016/j.celrep.2019.10.034.
37. Vlastaridis, P.; Kyriakidou, P.; Chaliotis, A.; Van de Peer,

- Y.; Oliver, S.G.; Amoutzias, G. D. *Gigascience* **2017**, 6, giw015, DOI: 10.1093/gigascience/giw015.
38. Macek, B.; Mijakovic, I.; Olsen, J. V.; Gnad, F.; Kumar, C.; Jensen, P. R.; Mann, M. *Mol. Cell. Proteom.* **2007**, 6, 697, DOI: 10.1074/mcp.M700311-MCP200.
39. Chen, D.; Shen, X.; Sun, L. *Anal. Chim. Acta* **2018**, 1012, 1, DOI: 10.1016/j.aca.2018.01.037.
40. Cohen, P. *Nat. Cell Biol.* **2002**, 4, E127, DOI: 10.1038/ncb0502-e127.